Electronic Supplementary Material (ESI) for Physical Chemistry Chemical Physics.

Quantum chemistry on quantum computers: Quantum simulations of the time evolution of wave functions under the S^2 operator and determination of the spin quantum number *S*

by

Kenji Sugisaki,[*a] Shigeaki Nakazawa,[†a] Kazuo Toyota,[a] Kazunobu Sato,[*a] Daisuke Shiomi[a] and Takeji Takui[*a,b]

[a.] Department of Chemistry and Molecular Materials Science, Graduate School of Science, Osaka City University, 3-3-138 Sugimoto, Sumiyoshi-ku, Osaka 558-8585, Japan. E-mail: sugisaki@sci.osaka-cu.ac.jp, sato@sci.osaka-cu.ac.jp, takui@sci.osaka-cu.ac.jp

[b.] Research Support Department/University Research Administrator Center, Unviersity Administration Division, Osaka City University, 3-3-138 Sugimoto, Sumiyoshi-ku, Osaka 558-8585, Japan.

[†] Ceased on March 23, 2019.

Table of Contents

1. Definitions of quantum gates

In the current implementations of quantum circuits, we use the following quantum gates as the building blocks, all of them are available as the default quantum gates in Cirq package: Hadamard gate H_d, Phase shift gate Z^{θ}, controlled phase shift gate CZ^{θ}, controlled-NOT (CNOT) gate, Toffoli (CCNOT) gate, and controlled-controlled-rotation (CCX^{θ}) gate. The corresponding circuit symbols and matrix representations of these quantum gates are summarized in Table S1.

Table S1. Graph and matrix representations of quantum gates.

Gate	Circuit symbols	Matrix representations[a]
H_d	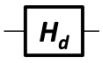	$\frac{1}{\sqrt{2}}\begin{pmatrix}1 & 1\\ 1 & -1\end{pmatrix}$
Z^{θ}		$\begin{pmatrix}1 & 0\\ 0 & \exp(i\pi\theta)\end{pmatrix}$
CZ^{θ}	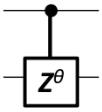	$\begin{pmatrix}1 & 0 & 0 & 0\\ 0 & 1 & 0 & 0\\ 0 & 0 & 1 & 0\\ 0 & 0 & 0 & \exp(i\pi\theta)\end{pmatrix}$
CNOT	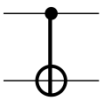	$\begin{pmatrix}1 & 0 & 0 & 0\\ 0 & 1 & 0 & 0\\ 0 & 0 & 0 & 1\\ 0 & 0 & 1 & 0\end{pmatrix}$
Toffoli	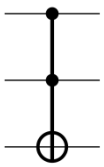	$\begin{pmatrix}1 & 0 & 0 & 0 & 0 & 0 & 0 & 0\\ 0 & 1 & 0 & 0 & 0 & 0 & 0 & 0\\ 0 & 0 & 1 & 0 & 0 & 0 & 0 & 0\\ 0 & 0 & 0 & 1 & 0 & 0 & 0 & 0\\ 0 & 0 & 0 & 0 & 1 & 0 & 0 & 0\\ 0 & 0 & 0 & 0 & 0 & 1 & 0 & 0\\ 0 & 0 & 0 & 0 & 0 & 0 & 0 & 1\\ 0 & 0 & 0 & 0 & 0 & 0 & 1 & 0\end{pmatrix}$
CCX^{θ}	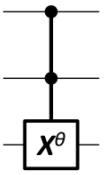	$\begin{pmatrix}1 & 0 & 0 & 0 & 0 & 0 & 0 & 0\\ 0 & 1 & 0 & 0 & 0 & 0 & 0 & 0\\ 0 & 0 & 1 & 0 & 0 & 0 & 0 & 0\\ 0 & 0 & 0 & 1 & 0 & 0 & 0 & 0\\ 0 & 0 & 0 & 0 & 1 & 0 & 0 & 0\\ 0 & 0 & 0 & 0 & 0 & 1 & 0 & 0\\ 0 & 0 & 0 & 0 & 0 & 0 & c & -s\\ 0 & 0 & 0 & 0 & 0 & 0 & -s & c\end{pmatrix}$

[a] $c = \cos(\pi\theta/2)$, $s = \sin(\pi\theta/2)$

2. Quantum circuit simulations for the time evolution of wave functions under the S^2 operator

To simulate quantum circuits for the time evolutions of wave functions under the $\mathbf{S}^2$ operators ($\exp(-i\mathbf{S}^2t)|\Psi\rangle$), we have developed a python code using OpenFermion and Cirq programs. The quantum circuit simulations were performed with $t = 2\pi$ and 360 of Trotter slices ($t = 2\pi/360$ for a single Trotter step) at the first order Trotter decomposition, with various starting wave functions including the eigenfunctions of the $\mathbf{S}^2$ operator (hereafter denoted as the spin eigenfunctions) and spin-mixed wave functions (linear combinations of the spin eigenfunctions with different spin quantum numbers). From theory, if we used the spin eigenfunctions as the initial wave functions, applying the time evolution operator $\exp(-i\mathbf{S}^2t)$ causes global phase shift on the wave functions depending on their $\mathbf{S}^2$ eigenvalues (see eq (S1)) without changing the structure of wave functions, as given in eqs (S2)–(S5) for spin-singlet ($S = 0$), doublet ($S = 1/2$), triplet ($S = 1$), and quartet (S = 3/2) states, respectively, for example.

$$\exp(-i\mathbf{S}^2t)|\Psi(S)\rangle = \exp(-iS(S+1)t)|\Psi(S)\rangle \quad \text{(S1)}$$

$$\exp(-i\mathbf{S}^2t)|\Psi(S=0)\rangle = |\Psi(S=0)\rangle \quad \text{(S2)}$$

$$\exp(-i\mathbf{S}^2t)|\Psi(S=1/2)\rangle = \exp\left(-\tfrac{3}{4}it\right)|\Psi(S=1/2)\rangle \quad \text{(S3)}$$

$$\exp(-i\mathbf{S}^2t)|\Psi(S=1)\rangle = \exp(-2it)|\Psi(S=1)\rangle \quad \text{(S4)}$$

$$\exp(-i\mathbf{S}^2t)|\Psi(S=3/2)\rangle = \exp\left(-\tfrac{15}{4}it\right)|\Psi(S=3/2)\rangle \quad \text{(S5)}$$

If we use spin-mixed wave functions like $|\alpha\beta\rangle$ and $|\alpha\alpha\beta\rangle$ as described in the main text, the wave function components having different spin quantum numbers evolve differently, which cause interferences between the spin eigenfunctions and the state transforms e.g., from $|\alpha\beta\rangle$ to $|\beta\alpha\rangle$, and $|\alpha\alpha\beta\rangle$ to $|\alpha\beta\alpha\rangle$ and $|\beta\alpha\alpha\rangle$, as given in eqs (S6)–(S9).

$$|\alpha\beta\rangle = \tfrac{1}{\sqrt{2}}\left[\left\{\tfrac{1}{\sqrt{2}}(|\alpha\beta\rangle - |\beta\alpha\rangle)\right\} + \left\{\tfrac{1}{\sqrt{2}}(|\alpha\beta\rangle + |\beta\alpha\rangle)\right\}\right]$$

$$= \tfrac{1}{\sqrt{2}}\{|\Psi(S=0)\rangle + |\Psi(S=1)\rangle\} \quad \text{(S6)}$$

$$\exp(-i\mathbf{S}^2t)|\alpha\beta\rangle = \tfrac{1}{\sqrt{2}}\{\exp(-i\mathbf{S}^2t)|\Psi(S=0)\rangle + \exp(-i\mathbf{S}^2t)|\Psi(S=1)\rangle\}$$

$$= \tfrac{1}{\sqrt{2}}\{|\Psi(S=0)\rangle + \exp(-2it)|\Psi(S=1)\rangle\}$$

$$= \tfrac{1}{\sqrt{2}}\left[\left\{\tfrac{1}{\sqrt{2}}(|\alpha\beta\rangle - |\beta\alpha\rangle)\right\} + \exp(-2it) \times \left\{\tfrac{1}{\sqrt{2}}(|\alpha\beta\rangle + |\beta\alpha\rangle)\right\}\right]$$

$$= \tfrac{1}{2}\{\exp(-2it)+1\}|\alpha\beta\rangle + \tfrac{1}{2}\{\exp(-2it)-1\}|\beta\alpha\rangle \quad \text{(S7)}$$

$$|\alpha\alpha\beta\rangle = \tfrac{\sqrt{2}}{\sqrt{3}}\left\{\tfrac{1}{\sqrt{6}}(2|\alpha\alpha\beta\rangle - |\alpha\beta\alpha\rangle - |\beta\alpha\alpha\rangle)\right\} + \tfrac{1}{\sqrt{3}}\left\{\tfrac{1}{\sqrt{3}}(|\alpha\alpha\beta\rangle + |\alpha\beta\alpha\rangle + |\beta\alpha\alpha\rangle)\right\}$$

$$= \frac{\sqrt{2}}{\sqrt{3}}|\Psi(S=1/2)\rangle + \frac{1}{\sqrt{3}}|\Psi(S=3/2)\rangle \tag{S8}$$

$$\exp(-i\mathbf{S}^2 t)|\alpha\alpha\beta\rangle = \frac{\sqrt{2}}{\sqrt{3}}\exp(-i\mathbf{S}^2 t)|\Psi(S=1/2)\rangle + \frac{1}{\sqrt{3}}\exp(-i\mathbf{S}^2 t)|\Psi(S=3/2)\rangle$$

$$= \frac{\sqrt{2}}{\sqrt{3}}\exp\left(-\frac{3}{4}it\right)|\Psi(S=1/2)\rangle + \frac{1}{\sqrt{3}}\exp\left(-\frac{15}{4}it\right)|\Psi(S=3/2)\rangle$$

$$= \frac{1}{3}\exp\left(-\frac{3}{4}it\right)(2|\alpha\alpha\beta\rangle - |\alpha\beta\alpha\rangle - |\beta\alpha\alpha\rangle)$$

$$+\frac{1}{3}\exp\left(-\frac{15}{4}it\right)(|\alpha\alpha\beta\rangle + |\alpha\beta\alpha\rangle + |\beta\alpha\alpha\rangle)$$

$$= \frac{1}{3}\left\{2\exp\left(-\frac{3}{4}it\right) + \exp\left(-\frac{15}{4}it\right)\right\}|\alpha\alpha\beta\rangle$$

$$+\frac{1}{3}\left\{-\exp\left(-\frac{3}{4}it\right) + \exp\left(-\frac{15}{4}it\right)\right\}(|\alpha\beta\alpha\rangle + |\beta\alpha\alpha\rangle) \tag{S9}$$

The quantum circuit simulation results of $\exp(-i\mathbf{S}^2 t)|\Psi\rangle$ using spin-singlet and triplet eigenfunctions are illustrated in Figures S1 and S2, respectively. In Figures S1 and S2, we plotted the real and imaginary part of the coefficients of $|\alpha\beta\rangle$ and $|\beta\alpha\rangle$ determinants. Clearly the time evolution by the $\mathbf{S}^2$ operator does not change the global phase of spin-singlet wave function. By contrast, the spin-triplet wave function gains the global phase through the time evolution under the $\mathbf{S}^2$ operator. We calculated the overlap between the simulated wave function and the wave function under the exact time evolution $\langle\Psi_{sim}(t)|\Psi_{exact}(t)\rangle$, finding that the overlap is larger than 0.9999996 everywhere.

For three molecular orbital systems, we have carried out quantum circuit simulations of the time evolution using several different initial wave functions: A three-spin doublet wave function, quartet wave function, and spin-triplet wave function consisting of two Slater determinants as given in eqs (S10)–(S12), respectively.

$$|\Psi(S=1/2)\rangle = \frac{1}{\sqrt{6}}(2|\alpha\alpha\beta\rangle - |\alpha\beta\alpha\rangle - |\beta\alpha\alpha\rangle) \tag{S10}$$

$$|\Psi(S=3/2)\rangle = \frac{1}{\sqrt{3}}(|\alpha\alpha\beta\rangle + |\alpha\beta\alpha\rangle + |\beta\alpha\alpha\rangle) \tag{S11}$$

$$|\Psi(S=1)\rangle = \frac{\sqrt{3}}{2}|2\alpha\alpha\rangle - \frac{1}{2}|\alpha 2\alpha\rangle \tag{S12}$$

The results of the quantum circuit simulations are depicted in Figures S3–S5 for the initial wave functions given in eqs (S10)–(S12), respectively. In all the cases under study the initial wave functions are the spin eigenfunctions and therefore only the global phase shift can be observed. In all the cases we obtained $\langle\Psi_{sim}(t)|\Psi_{exact}(t)\rangle > 0.9999996$.

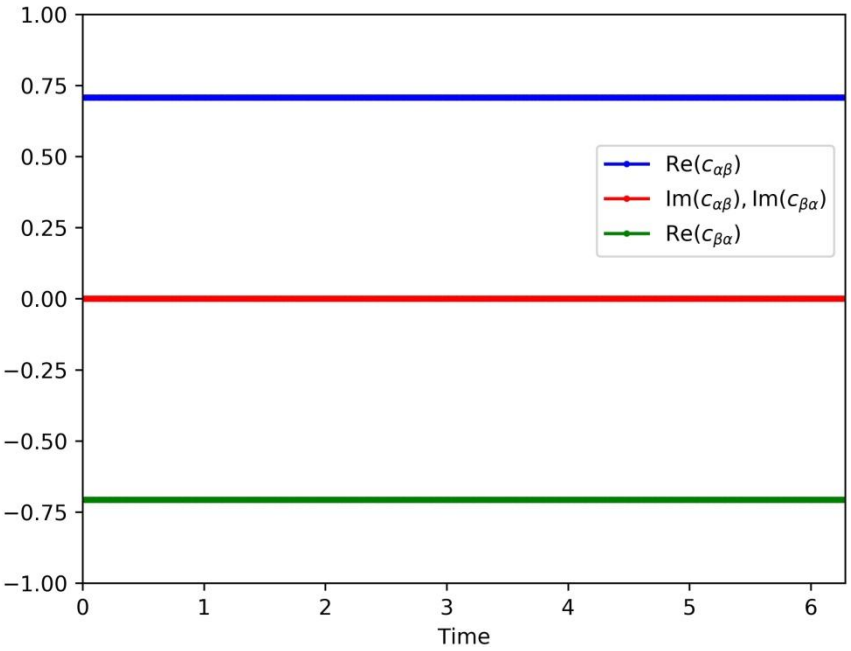

Figure S1. The real and imaginary part of the coefficients of |αβ⟩ and |βα⟩ determinants ($c_{\alpha\beta}$ and $c_{\beta\alpha}$, respectively), in the time evolution under the $\mathbf{S}^2$ operator starting from the spin-singlet wave function $|\Psi(S=0)\rangle = \frac{1}{\sqrt{2}}(|\alpha\beta\rangle - |\beta\alpha\rangle)$.

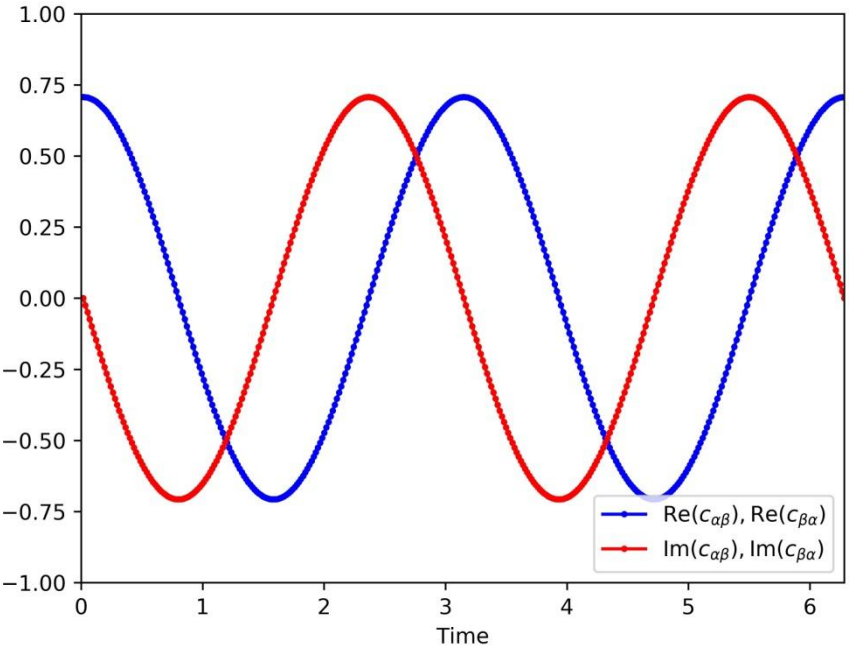

Figure S2. The real and imaginary part of the coefficients of |αβ⟩ and |βα⟩ determinants ($c_{\alpha\beta}$ and $c_{\beta\alpha}$, respectively), in the time evolution under the $\mathbf{S}^2$ operator starting from the spin-triplet wave function $|\Psi(S=1)\rangle = \frac{1}{\sqrt{2}}(|\alpha\beta\rangle + |\beta\alpha\rangle)$.

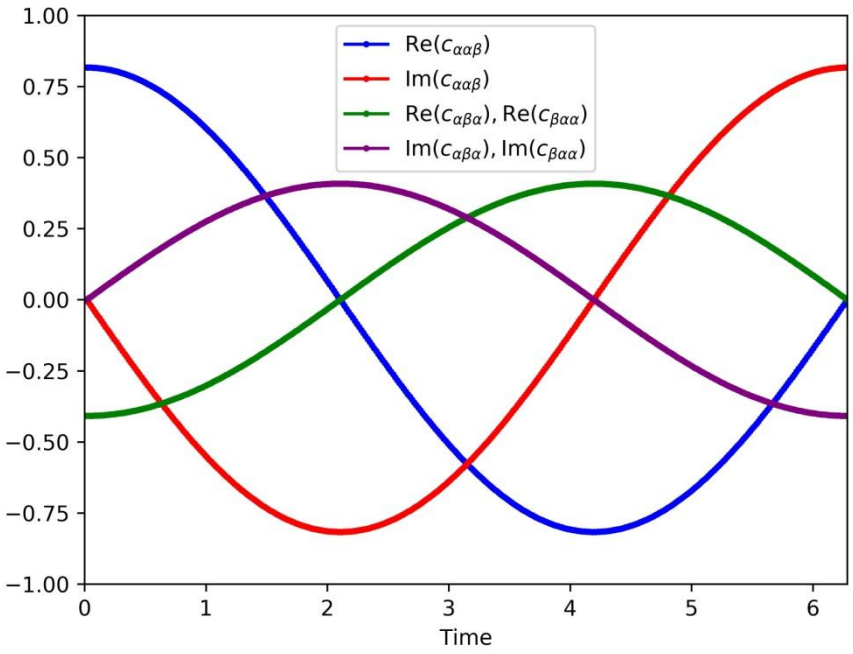

Figure S3. The real and imaginary part of the coefficients of $|\alpha\alpha\beta\rangle$, $|\alpha\beta\alpha\rangle$, and $|\beta\alpha\alpha\rangle$ determinants ($c_{\alpha\alpha\beta}$, $c_{\alpha\beta\alpha}$, and $c_{\beta\alpha\alpha}$, respectively), in the time evolution under $\mathbf{S}^2$ operator starting from the three-spin doublet wave function $|\Psi(S=1/2)\rangle = \frac{1}{\sqrt{6}}(2|\alpha\alpha\beta\rangle - |\alpha\beta\alpha\rangle - |\beta\alpha\alpha\rangle)$.

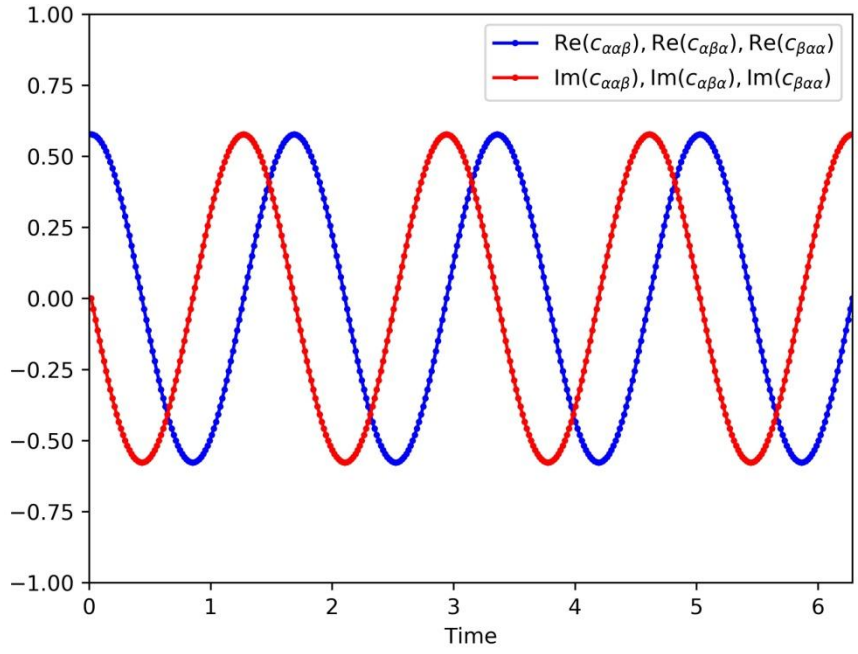

Figure S4. The real and imaginary part of the coefficients of $|\alpha\alpha\beta\rangle$, $|\alpha\beta\alpha\rangle$, and $|\beta\alpha\alpha\rangle$ determinants ($c_{\alpha\alpha\beta}$, $c_{\alpha\beta\alpha}$, and $c_{\beta\alpha\alpha}$, respectively), in the time evolution under $\mathbf{S}^2$ operator starting from the spin quartet wave function $|\Psi(S=3/2)\rangle = \frac{1}{\sqrt{3}}(|\alpha\alpha\beta\rangle + |\alpha\beta\alpha\rangle + |\beta\alpha\alpha\rangle)$.

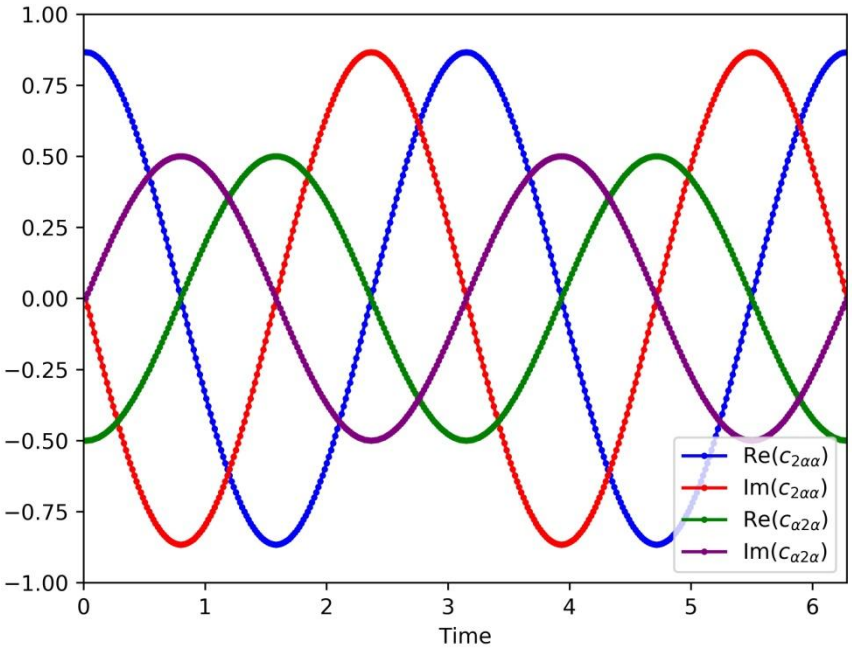

Figure S5. The real and imaginary part of the coefficients of |2αα⟩ and |α2α⟩ determinants ($c_{2\alpha\alpha}$ and $c_{\alpha 2\alpha}$, respectively), in the time evolution under $\mathbf{S}^2$ operator starting from the spin quartet wave function $|\Psi(S=1)\rangle = \frac{\sqrt{3}}{2}|2\alpha\alpha\rangle - \frac{1}{2}|\alpha 2\alpha\rangle$.

3. Quantum circuit simulations for the quantum phase estimations to determine the S^2 eigenvalue

For the quantum circuit simulations of the quantum phase estimation (QPE) to determine $\mathbf{S}^2$ eigenvalues, we have developed python codes using OpenFermion and Cirq. QPE requires controlled-U operations where $U = \exp(-i\mathbf{S}^2 t)$ in our case (see Figure 4 in the main text). The quantum circuit for QPE simulations of two molecular orbital systems such as a H_2 molecule in the minimal basis is given in Figure S6. We used controlled phase shift operations, in which the qubit used for the QPE measurement is settled as the control qubit to realize controlled-U operations. To implement QPE with $U = \exp(-i\mathbf{S}^2 t)$ in conjunction with the GSCM, we have to implement control-control-control-X^{θ} (CCC-X^{θ}) operations. We substituted CCC-X^{θ} operations for two Toffoli (CCNOT) and one CC-X^{θ} operations.

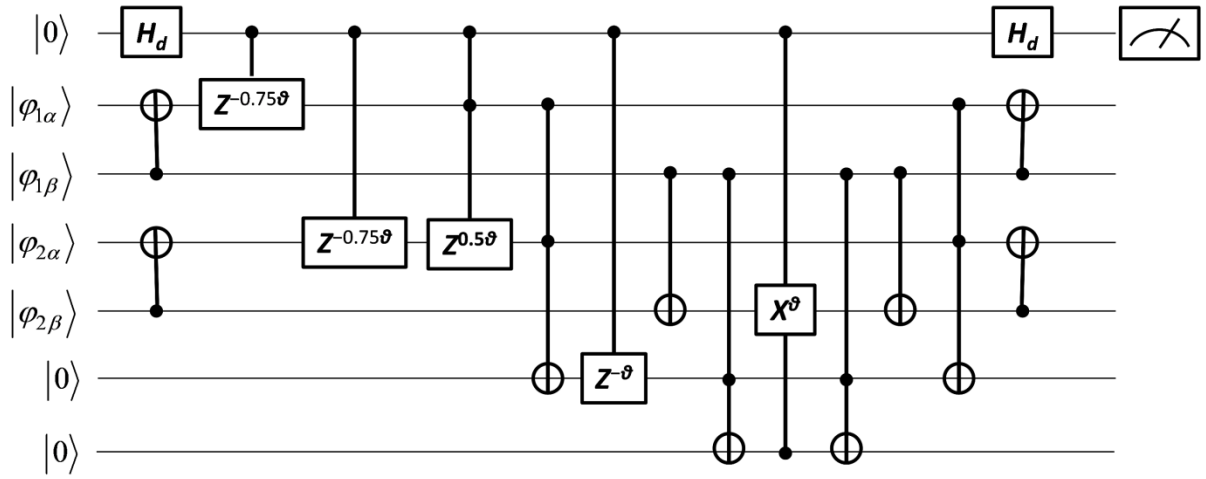

Figure S6. A quantum circuit for one-qubit quantum phase estimation in two molecular orbital systems like a H_2 molecule in the minimal basis.

The quantum circuit simulations of QPE for two-electron systems are given in the main text. Here, we describe the numerical simulations of QPE for three electron systems with the spin quantum number S = 3/2 and 1/2. As given in eqs (3) and (5), the $\mathbf{S}^2$ eigenvalues of S = 3/2 and S = 1/2 states are 15/4 and 3/4, respectively. The probability to get the $|1\rangle$ state in the measurement becomes maximum at the time when $\exp(-i\mathbf{S}^2 t) = -1$, and therefore we will always get the $|1\rangle$ state at $t = 4x\pi/15$ and $t = 4x\pi/3$ for S = 3/2 and S = 1/2, respectively, where x is an odd natural number.

Results of the quantum circuit simulations of QPE using three-spin doublet and quartet wave functions are summarized in Figure S7. In Figure S7, we gradually changed evolution time from 0 to 2π, and performed the QPE simulations without the phase shift operation Z^{η} appearing after the control-U operation in Figure 4 in the main text. Time for the single Trotter step was set to be π/360. To calculate the probability we carried out quantum circuit simulations 10,000 times for each simulation time. As expected, the probability to obtain the $|1\rangle$ state became maximum at the evolution time t = 4π/15, 4π/5, 4π/3, and

$28\pi/15$ in the simulations of the spin-quartet wave function. For the spin-doublet wave function, the maximum probability was obtained at time $t = 4\pi/3$.

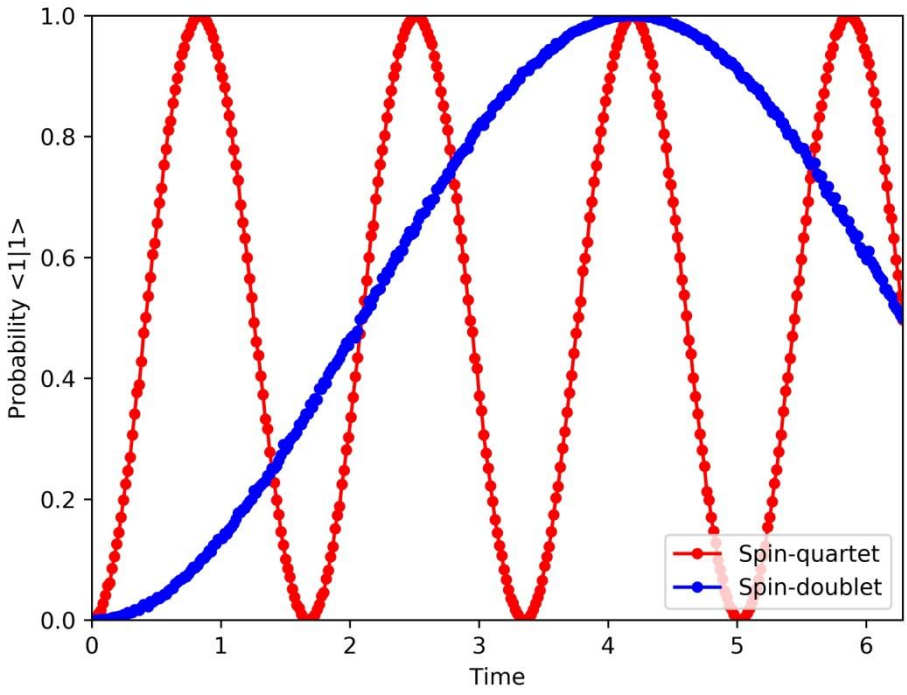

Figure S7. Quantum circuit simulation results of the QPE in three-electron systems without the phase shift operation Z^{η} in Figure 4 in the main text.

To calculate the spin quantum number of three-electron systems on quantum computers in a deterministic manner using one qubit for QPE, simple QPE circuits are not enough and we have to introduce a phase shift operation Z^{η} after the controlled-U operation, as illustrated in Figure 4 in the main text. The Z^{η} operation shifts the phase of the $|1\rangle$ state by a factor $\exp(i\pi\eta)$, and therefore QPE simulations with the Z^{η} operation corresponds to use an $(\mathbf{S}^2 - \eta\pi\mathbf{1})$ operator instead of $\mathbf{S}^2$, where $\mathbf{1}$ denotes an identity operator. By setting the rotation angle $\eta = \frac{3}{4\pi}t$, we can always obtain the $|0\rangle$ state for the spin-doublet wave function. The quantum circuit simulation results of the QPE in three-spin systems with the phase shift operation Z^{η} in Figure 4 with $\eta = \frac{3}{4\pi}t$ are given in Figure S8. From the simulation results, clearly we can discriminate the spin-doublet and quartet wave functions in a deterministic manner by applying $t = \pi/3$ and $\eta = 1/4$. Addition of the phase shift operation Z^{η} is useful for the study of odd electron systems. We also performed QPE simulations with $t = \pi/3$ and $\eta = 1/4$ by using the spin-mixed wave function $|\alpha\alpha\beta\rangle$, which is a 2:1 mixture of spin-doublet and quartet wave functions as given in eq (S13) as the initial wave function. The QPE simulations gave $|1\rangle$ state 33,250 times out of 100,000 repetitive simulations, which is very close to the ideal probability 1/3.

$$|\alpha\alpha\beta\rangle = \frac{\sqrt{2}}{\sqrt{3}}|\Psi(S = 1/2)\rangle + \frac{1}{\sqrt{3}}|\Psi(S = 3/2)\rangle \quad \text{(S13)}$$

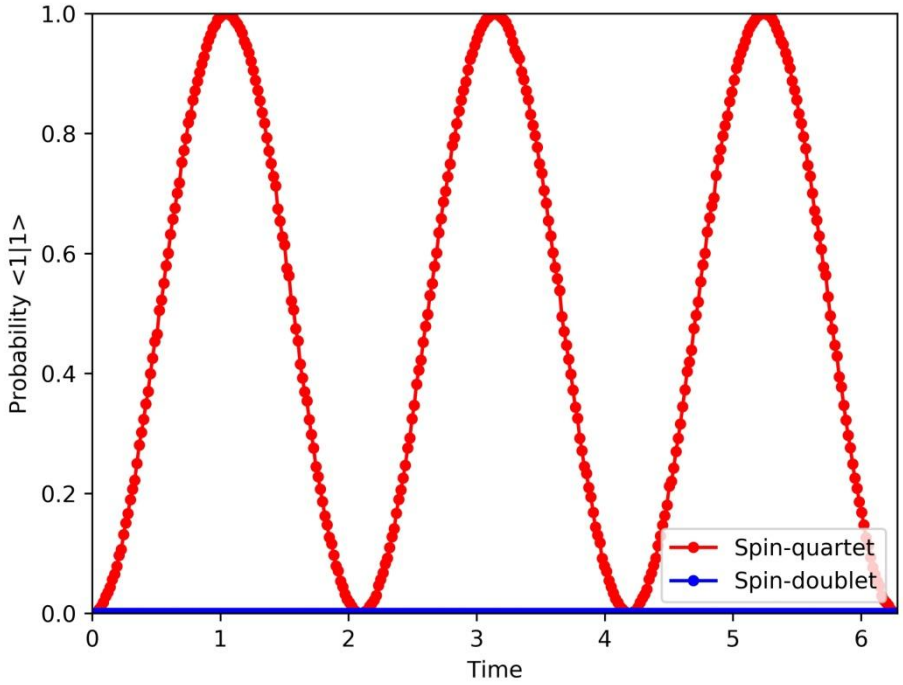

Figure S8. Quantum circuit simulation results of the QPE in three-electron systems with a phase shift operation Z^{η} ($\eta = \frac{3}{4\pi}t$) in Figure 4 in the main text.